Title	Gravity-induced shear force in reinforced concrete walls above transfer structures
Author(s)	Tang, TO; Su, RKL
Citation	Proceedings of the Institution of Civil Engineers: Structures and Buildings, 2015, v. 168 n. 1, p. 40-55
Issued Date	2015
URL	http://hdl.handle.net/10722/211729
Rights	Permission is granted by ICE Publishing to print one copy for personal use. Any other use of these PDF files is subject to reprint fees; This work is licensed under a Creative Commons Attribution-NonCommercial-NoDerivatives 4.0 International License.

Gravity-induced shear force in reinforced concrete walls above transfer structures

1 Tim On Tang BEng
PhD Candidate, Department of Civil Engineering, The University of
Hong Kong, Hong Kong, PRC

2 Ray Kai Leung Su BSc(Eng), PhD, CEng, MIStructE, MHKIE,
RPE(HK)
Associate Professor, Department of Civil Engineering, The University
of Hong Kong, Hong Kong, PRC

In this study, the gravity loads in reinforced concrete shear walls supported on transfer structures are investigated.
Emphasis is placed on the shear-stress concentration effects on the supported shear walls owing to the distortion of the
transfer structure. A simplified model is proposed to illustrate the fundamental physical interactions. Finite-element
analysis is also conducted to study the influences of the symmetric and asymmetric shear-wall arrangements,
positioning of supporting columns and span-to-depth ratio of the transfer structure. Non-linear behaviours encompass-
ing the use of yielded stiffness at ultimate limit state, sequential construction and the creep of reinforced concrete under
gravity loads are addressed. Various effects of modelling assumptions and simplifications on the stress redistribution of
the transfer structure are investigated. Remedial measures are proposed, such as increasing the depth of the transfer
girders using late-cast slabs, segmented upper shear walls and concrete of higher grade for critical regions.

Notation

A_i	gross sectional area of the ith wall
$A_{s,i}$	shear area of the ith wall
B	elastic compliance tensor
b	breadth of the wall
d	effective depth of the wall
d_i	total depth of the ith wall
E	short-term elastic modulus
E''	effective modulus accounting for creeping of RC
f'_c	mean cylinder strength of concrete
f_{ck}	characteristic cylinder strength of concrete
f_{cu}	characteristic cube strength of concrete
G	short-term shear modulus
I	gross moment of inertia
L	clear span of the transfer structure
M_i	moment load on the ith wall
n	total number of columns/walls in a storey
R	linear algebraic relaxation function
t	days elapse since first loading
t_0	days when first loading is applied
V_i	shear load on the ith wall
χ	ageing coefficient
$\Delta\sigma$ or $\Delta\varepsilon$	the change in strain or stress tensor from time t_0 to t
ε	strain tensor
ε_0	initial strain at the time of first loading
σ	stress tensor
$\sigma_{M,i}$	bending stress on the extreme fibre of the wall
$\sigma_{N,\,total}$	average normal stress of all walls on a storey
$\sigma_{V,i}$	average shear stress on the wall
φ	creep coefficient

1.   Introduction

High-rise buildings have become commonplace in developed and
densely populated cities due to advances in building technologies
over the last few decades. Among these buildings, transfer
structures, which distribute vertical loading from shear walls
above to widely spaced columns below through transfer girders or
plates, have prevailed because they can accommodate the compo-
site use of areas. However, critical shear stress and normal stress
on shear walls can arise from deformed transfer structures under
gravity loads. Such stress redistribution can result in severe shear
and moment loads on the supported shear walls with magnitudes
comparable to resultant forces under wind or seismic loads.
Without conducting the appropriate analysis of the full transfer
structure model, this fact could be overlooked by practising
engineers who have no prior knowledge of such effects.

Owing to the complexity of interaction between the transfer structure and supported walls, the latest physical model available is still based on the former arching theory proposed by Macleod and Green (1973) and Stafford Smith and Riddington (1977) for directly supported shear walls with columns below the transfer structure. Such a physical model assumes that the gravity loads are transferred from the supported shear walls to columns below through primary and secondary compression arches formed within the shear walls and the transfer structure, whereas the transfer girder in connection with the supported shear wall is simplified as a rigid arm. The latter assumption is a typical simplification in the frame analysis, yet it violates the actual phenomenon observed in the detailed finite-element analysis. When relatively thin shear walls are supported above a transfer girder much wider than the thickness of the wall, significant curvatures can be observed even in cross-sections under the wall. Omission of the curvature of a transfer girder would result in underestimating the base rotations of the walls and the resultant stresses induced in the walls and the coupling beams and slabs. In addition, loads from walls supported on a cantilever transfer girder are seldom transferred in the same way as a compression arch. Figure 1 shows some typical shear cracks on exterior walls and tension cracks on a slab and a coupling beam just above transfer structures, which cannot be explained by the existing arching

(a)

(b)

Figure 1. Cracked wall, slab and beam sections above the transfer level: (a) cracked walls above cantilevered transfer structures and (b) tension cracks on a slab and a coupling beam above the transfer level

Structures and Buildings
Volume 168 Issue SB1

Gravity-induced shear force in reinforced
concrete walls above transfer structures
Tang and Su

theory. Apart from thermal or shrinkage cracks, these extensive cracks on normal-sized reinforced concrete (RC) walls, beams and slabs under service are likely attributed to shear and bending concentrations in improperly designed structures. Precautions to control thermal and shrinkage cracking in bulky transfer structures have been discussed in various studies (e.g., Liu and Wang, 2009; Man, 2010). However, possible improper designs have rarely been mentioned. In these adverse circumstances, large induced shear loads could even dictate the structural design when the loads are combined with wind or seismic loads (Su and Cheng, 2008).

To quantify the stress concentration effect on coupled shear walls above a transfer structure, analogous physical models, such as a coupled shear wall supported on a flexible basis, have been reviewed. The study was first conducted by Coull (1971), who treated the vertical and rotational base flexibility separately by vertical and rotational springs. Based on the continuum approach for laterally loaded coupled shear walls, a closed-form solution was obtained by superimpositions of these results, which incorporates the foundation–structure interaction. Coull and Chantaksinopas (1974) extended the study to include symmetric coupled shear walls resting on an elastic foundation or above a portal frame hinged to a rigid ground. The latter model is more relevant to the current issue; yet, there are inherent assumptions including the fact that all the derivations are based on a laterally loaded system and that the point of contraflexure is formed at the mid-span of transfer girders. Obviously, this is not applicable to a gravity loaded system. Other similar studies have been conducted by various researchers such as Toutanji (1997) and Choo and Li (1997), who have respectively accounted for the base deformations of walls in the frame-wall system and the multi-stiffened coupled shear wall system. Latest developments have extended to studies of elasto-plastic behaviour using the discrete force method and assuming that plasticity is restricted to the coupling beams (Nadjai and Johnson, 1998). Those studies simulated the foundation–structure interaction by assigning separate vertical and rotational springs to the base of walls; their stiffnesses are associated with the ground properties. Not only is the constant stiffness assumed for soil grounds not applicable to transfer–shear wall interaction, as its stiffness depends on supporting transfer structures and varies along the position of the shear wall, but the difference in base rotational angles of adjacent walls also leads to a more significant shear concentration effect, which has been neglected in the aforementioned studies for the sake of simplicity (Coull, 1971; Toutanji, 1997). As coupled shear walls are mainly designed to resist lateral wind and seismic loads, most studies emphasise the lateral loads effect or the determination of the free vibration periods for seismic analysis (e.g., Vuddandam *et al.*, 2013). Kuang and Zhang (2003) conducted parametric studies to evaluate the stress concentration effect under gravity loads; however, these studies were limited to a continuous wall supported above the transfer structures, and the analysis was focused on uneven axial stress distributions along the wall–transfer interface. As a result, the shear stress concentrations on wall–transfer interaction owing to gravity loads are worth examining.

In this study, a comprehensive physical model describing the contribution of the slab and beams above the transfer structure and the deformed shapes of the adjacent columns and walls is proposed to illustrate the interaction effect of the transfer structure under in-plane gravity loads. Critical parameters contributing to the shear stress concentration are outlined and examined using parametric studies of numerical models. By comparing the average shear stresses induced on the wall–transfer interface in different situations, remedial actions in terms of revising the structural layouts and improving the modelling techniques are suggested as a design reference to practising engineers.

2. Formation of shear concentration under gravity loads

The presence of stiff and massive transfer structures can affect the displacement responses of a building under lateral or gravity loads. An abrupt change in the inter-storey drift and shear loads on the walls often occurs in the vicinity of the transfer level. Many engineers may ignore the out-of-plane deformations of the transfer plate, larger than the walls they support, and adopt rigid plate and rigid diaphragm assumptions in gravity load or lateral load calculations. However, such local deformations are the primary cause of the abrupt change in shear in exterior walls and should not be neglected in gravity load and lateral load analyses.

The effect of shear concentration on the transfer structure under lateral loads has been discussed by Su and Cheng (2008). The out-of-plane deformation of the transfer plate could result in shear concentration on the exterior walls above transfer structures. Figure 2 illustrates hogging and sagging deformations generated in the transfer structure owing to gravity loads.
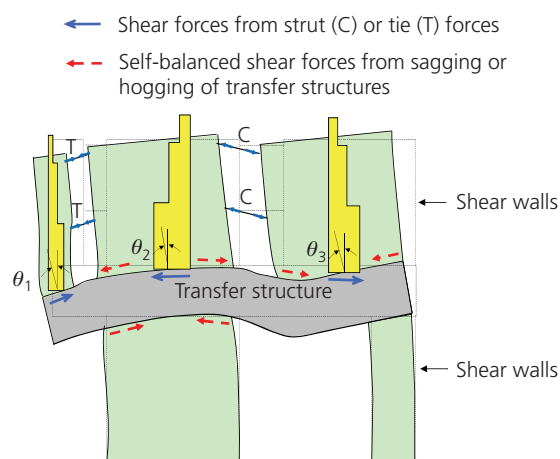

Figure 2. Local deformations and shear concentration of a transfer structure owing to gravity loads

Structures and Buildings
Volume 168 Issue SB1

Gravity-induced shear force in reinforced
concrete walls above transfer structures
Tang and Su

Relatively thin shear walls cannot constrain the out-of-plane deformation of transfer plate effectively. As the shear walls are connected monolithically to the transfer structure, the walls and transfer plate deform together at the wall–transfer structure interfaces owing to the displacement compatibility. Hogging or sagging curvatures of the transfer beams in plans parallel to the walls can elongate or shorten the cross-sectional depth of walls, which can be explained as follows: assume that the wall is 300 mm thick and the transfer beam is 1000 mm wide, as in the example that will be later referred to in Figure 3. In this situation the wall–transfer structure interface is not sufficiently rigid to resist the gravity loads without forming curvature on the transfer girder in plans parallel to the plan of the wall. Such curvature results in generating some local stresses on the ends of the walls due to displacement compatibility in the transversal direction. A pair of almost self-balanced shear forces (indicated as grey arrows in Figure 2) could be developed in each wall. Further-more, the joint of the transfer structure and the wall is rotated in a similar manner. The walls at the transfer level rotate by different degrees and in different directions as vertical cantile-vers. However, as the horizontal movements of walls above the transfer levels are constrained by floor slabs and coupling beams, in-plane compressive or tensile restraining forces are generated in the slabs and beams. These horizontal reactions (indicated as black arrows in Figure 2) transmitted from one wall to the other walls are the origin of the abrupt change of shear forces and the shear concentration near the transfer level.

The above physical model indicates the amount of horizontal reaction generated depends on the lateral stiffnesses of the walls and the differences between their base rotations. Shear failure may occur in exterior walls, especially when it is offset from the support below at a significant distance. Moreover, slabs can be impaired by the high tensile stresses when the connecting walls rotate in the opposite direction. These predictions coincide with the observed cracks that occur in buildings with a cantilever transfer structure, as shown in Figure 1. As a consequence of the shear concentration effect, it is crucial to check the shear capacity of the walls and the shear demands to avoid unintentional shear failure of the walls. Nonetheless, the provisions for shear design, and in particular to the walls, are not well elaborated upon in most codes of practice. For comparison, the ultimate allowable design shear strength for RC columns and walls stipulated in Eurocode 2 (BS EN 1992–1-1, BSI, 2004), American Standards (ACI 318–11 (ACI, 2011)), New Zealand Standards (NZS 3101 (SNZ, 2006)), Canadian Standards (CSA A23.3–04 (CSA, 2004))
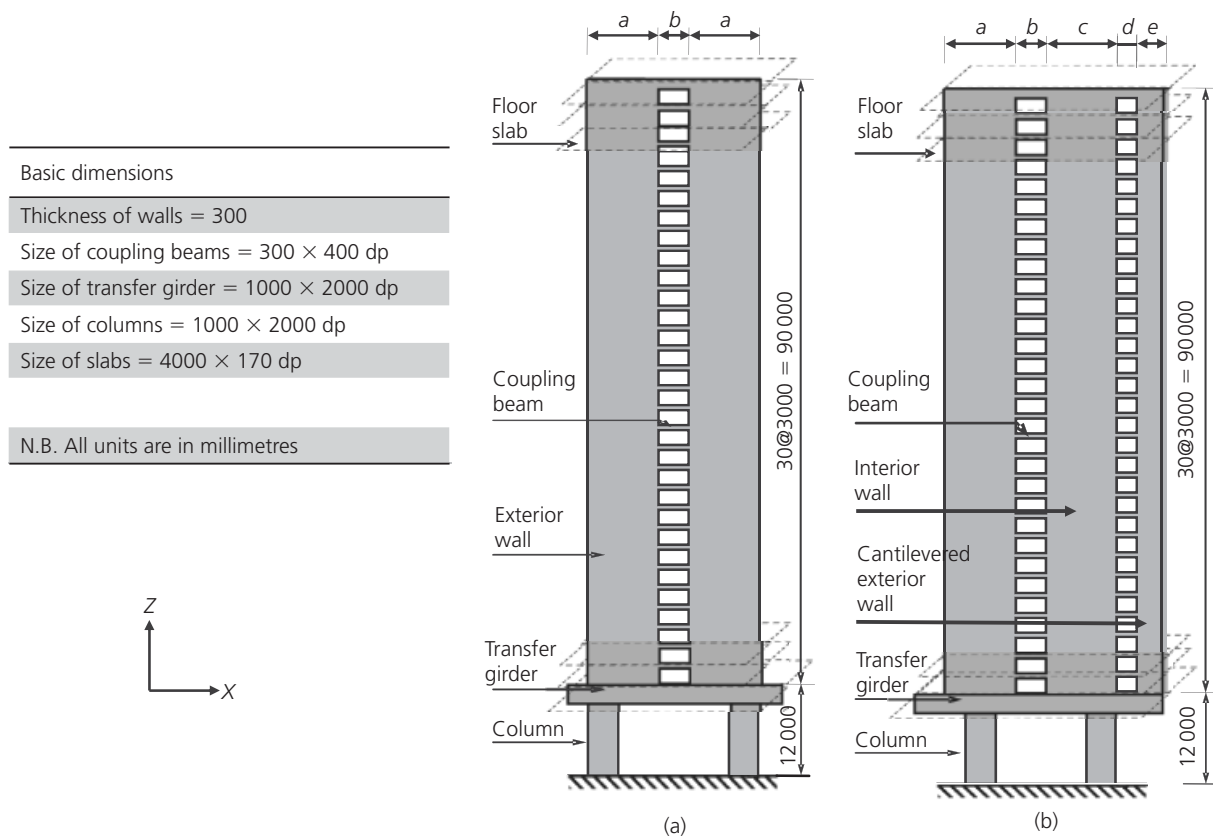

Figure 3. Typical structural arrangements of the numerical model: (a) model A with a symmetrical layout and (b) model B with an exterior wall on the cantilever girder support

Structures and Buildings
Volume 168 Issue SB1

Gravity-induced shear force in reinforced
concrete walls above transfer structures
Tang and Su

and the earlier British Standards (BS 8110 (BSI, 1997)) are summarised in Table 1. This design limit is codified to primarily guard against diagonal compression failure of the concrete strut in the truss analogy. Table 2 shows the shear stress limits for different concrete grades using the codified design equations, which increase with concrete grade and are limited to approximately 4 to 5 MPa by most codes of practice.

When extensive parametric studies are conducted, the critical interfacial shear stress on the wall–transfer joint can often reach 2 MPa or more. As a result, a considerable amount of interfacial shear stress has to be accounted for in the shear wall design even before the wind or seismic loads are introduced. This illustrates the significance of investigating this physical phenomenon.

In the following sections, finite-element models simulating the in-plane loaded shear walls above a transfer structure under gravity loads are presented. Factors influencing the shear concentration effect will be investigated. Thus effective alternatives can be identified to mitigate the shear concentration problem under gravity loads.

3. Computational modelling

To illustrate the shear stress concentration for upper shear walls and quantify various factors influencing such effects, two typical layouts of coupled shear walls on transfer girder models, as shown in Figure 3, are considered in the analysis. In the first model, two shear walls, coupled by beams and slabs, are

Concrete grade	C35	C40	C45	C50	C55	C60
f_{cu}: MPa	35	40	45	50	55	60
$f_{ck} = 0.8 f_{cu}$: MPa	28	32	36	40	44	48
Maximum design shear stress limit: MPa						
BS 8110 (BSI, 1997)	4·7	5·0	5·0	5·0	5·0	5·0
EC2 EN1992 (BSI, 2004)	5·0	5·6	6·2	6·7	7·3	7·8
ACI 318–11 (ACI, 2011)	3·3	3·5	3·7	3·9	4·1	4·3
CSA A.23.3–04 (CSA, 2004)	4·1	4·7	5·3	5·9	6·4	7·0
NZS 3101 (SNZ, 2006)	4·2	4·8	5·4	6·0	6·0	6·0

Table 2. Maximum design shear strength of various concrete grades

supported by a frame with a transfer girder. The second model consists of an additional exterior wall situated on the cantilevered transfer girder. This mimics the adverse effect in particular to this exterior wall owing to reversed rotations induced at the bases of the walls above the deformed transfer girder.

Both building models are 102 m high, comprising 30 typical floors above a transfer girder with an elevation of 12 m. Other basic dimensions of the models are shown in Figure 3 and Table 3. The material properties adopted in the analysis are shown in Table 4. Apart from the self-weight of 24·5 kN/m^3 for the RC material, a superimposed dead load of 6 kPa and a live load of

Codes of practice	Shear limit for RC columns and walls
BS 8110 (BSI, 1997)	The RC column follows beam shear design and is limited by the lesser of $0.8\sqrt{f_{cu}}$ and 5 MPa with a material factor of safety (FOS) $= 1.25$ considered, where f_{cu} is the characteristic cube strength of concrete. In contrast, there is no specific provision for the shear design of the wall.
EC2 EN1992 (BSI, 2004)	The shear strength design of all RC members is limited to $0.2[1 - f_{ck}/250] \times f_{ck}$, where f_{ck} is the characteristic cylinder strength of concrete in MPa. A material FOS $= 1.5$ is considered under transient loads.
ACI 318–11 (ACI, 2011)	A special provision for shear design in walls is specified. The maximum shear stress is limited to design strength $= 0.83\sqrt{f_{ck}} \times \phi$, where $\phi = 0.75$ is the strength reduction factor for shear (i.e., the material FOS $= 1.33$ for shear); $\sqrt{f_{ck}}$ should not exceed 8·3 MPa. The provision for beams and columns is similar to the above design value for non-prestressed members, without consideration of the axial load effect on the concrete shear strength.
CSA A23.3–04 (CSA, 2004)	For non-prestressed members, the maximum design shear stress $V_{r,max}$ shall not exceed $0.225 f_{ck} \times \phi_c$, where the shear cross section defined by effective shear depth $d_v = 0.9d$ is considered, and ϕ_c is the resistance factor for concrete $= 0.65$ (i.e., the material FOS $= 1.54$).
NZS 3101 (SNZ, 2006)	For column and pier design, the maximum design shear stress shall not exceed $0.2 f_{ck} \times \phi$ or $8 \times \phi$ MPa, where ϕ is the strength reduction factor $= 0.75$ (i.e., the material FOS $= 1.33$ for shear).

Notes: The strength reduction factor in ACI and NZS accounts for (a) the possible under-strength of members, (b) inaccuracies in design equations, (c) the importance and degree of ductility and reliability of members.

Table 1. Probable maximum design shear strength of RC columns and walls

Structures and Buildings
Volume 168 Issue SB1

Gravity-induced shear force in reinforced
concrete walls above transfer structures
Tang and Su

Model	Wall length			Coupling beam length		Total length: m
	a: m	*c*: m	*e*: m	*b*: m	*d*: m	
A	6	N.A.	N.A.	2	N.A.	14
B	6	5	2	2	1	16

Table 3. Dimensions of models

Property	Value
Concrete grade	45 MPa
Poisson ratio	0·2
Modulus of elasticity (*E*)	26·4 MPa

Table 4. Material properties of models

2 kPa, representing the typical loading on residential buildings, are adopted in the analysis. The resulting floor mass density of 5·89 kN/m³ is comparable to 5·5 kN/m³, which is the average density of typical residential blocks sampled in Hong Kong (Su *et al.*, 2003).

Owing to the complexities of the interaction between the supported shear walls and the transfer girder, the finite-element program Etabs (CSI, 2005) is employed for the analysis. Figure 4 shows the configuration of the models, in which shell elements are adopted for modelling support columns, upper shear walls, the transfer girder and slabs, while the coupling beams are modelled by frame elements. The shell elements are quadrilateral plane-stress elements with a constant mesh size of 250 mm. This discretisation was considered to yield accurate results, as reduction in the mesh size by 20% results in variations of less than 1% on the calculated shear and moment loads at the critical wall sections in models A and B.

Variables that influence the shear concentration effect comprising wall locations, depth of transfer girder and various modelling simplifications are considered in the present study. Non-linear
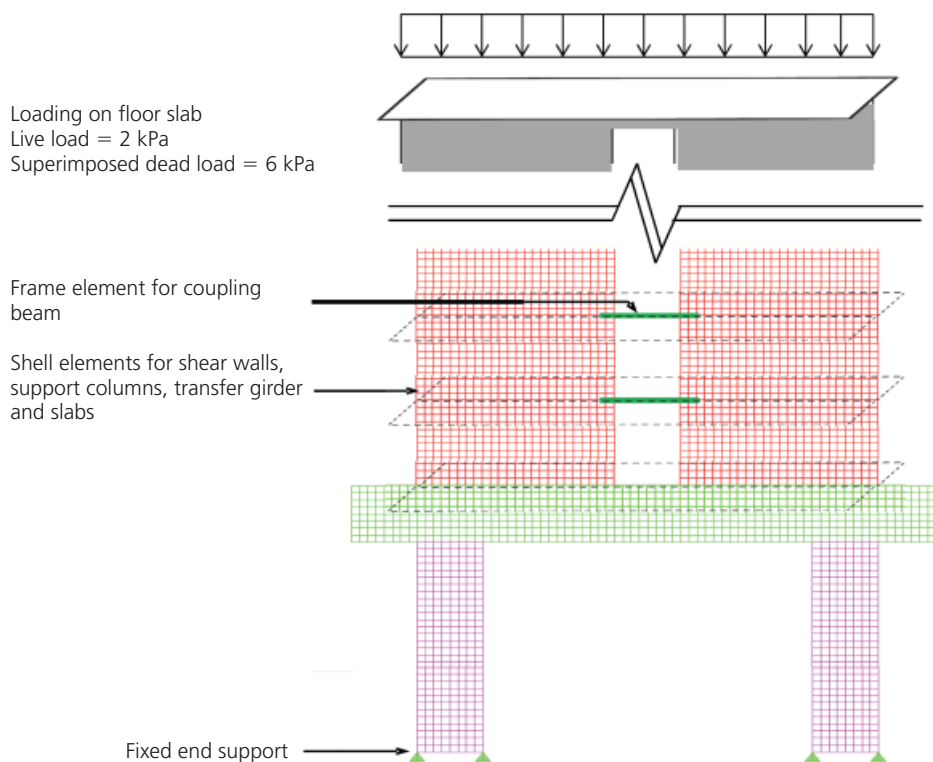

Figure 4. Finite-element model for coupled shear walls above the transfer girder

influences by the cracked sections, the stages of construction and the creeping of RC are discussed in Sections 4.6 and 4.7.

4. Results and discussions

4.1 Shear concentration on shear walls

Under long-term service loads, the vertical deflection-to-span ratio for the transfer girder in model A and model B conforms well to the permissible deflection limit of 1/480 for slabs, so as to avoid impairing any supported non-structural components (Table 9.5(b) of ACI 318–11 (ACI, 2011)). To assess the shear concentration on the walls and columns under the ultimate limit state, a shear concentration ratio (SCR) is defined in Equation 1

$$1. \quad \mathrm{SCR}_{i,j} = \left[\frac{V_i/A_{\mathrm{s},i}}{\left(\sum_{i=1}^{n} N_i\right) / \left(\sum_{i=1}^{n} A_i\right)} \right]_{j\mathrm{thfloor}}$$

$$2. \quad \mathrm{SCR}_{i,j} = \left[\frac{\sigma_{V,i}}{\sigma_{N,\mathrm{total}}} \right]_{j\mathrm{thfloor}}$$

where N_i and V_i are, respectively, the axial and shear loads on the ith wall, A_i denotes the gross sectional area and $A_{\mathrm{s},i}$ denotes the shear area equal to the product of the breadth (b) and the effective depth (d) of the wall. Alternatively, the SCR can be expressed as a dimensionless ratio of the shear stress ($\sigma_{V,i}$) on the ith wall to the average normal stress ($\sigma_{N,\mathrm{total}}$) of the total n number of walls on the jth floor. It is defined at different levels along the building height. The effective depth for the wall is further assumed herein as 0·8 times the total depth of the wall (d_i), which is recommended by ACI 318–11 (ACI, 2011) for preliminary assessments without a strain compatibility analysis of the section. Similarly, the warping of transfer structure induces in-plane moments on the supported walls. It is expressed as a bending concentration ratio (BCR), of which the bending stress on the extreme fibre ($\sigma_{M,i}$) is normalised by the average normal stress, $\sigma_{N,\mathrm{total}}$, provided that the elastic plane section is assumed. Hence, the BCR can be presented as Equation 3 or Equation 4.

$$3. \quad \mathrm{BCR}_{i,j} = \left[\frac{6M_i/bd_i^2}{\left(\sum_{i=1}^{n} N_i\right) / \left(\sum_{i=1}^{n} A_i\right)} \right]_{j\mathrm{thfloor}}$$

$$4. \quad \mathrm{BCR}_{i,j} = \left[\frac{\sigma_{M,i}}{\sigma_{N,\mathrm{total}}} \right]_{j\mathrm{thfloor}}$$

in which M_i is the moment load on the ith wall and d_i denotes the depth of the section. Similarly, the BCR can be expressed as a dimensionless ratio of the bending stress ($\sigma_{M,i}$) on the ith

wall to the average normal stress ($\sigma_{N,\mathrm{total}}$) of all walls and columns on the jth floor. Presuming all supported walls share similar axial stresses and the gravity load is transferred through a 45° inclined strut developed in the wall and transfer girder, the maximum induced shear stress would likely be limited by $1/0\cdot8 = 1\cdot25$ from Equation 1, where the factor 0·8 accounts for the effective shear area. The value of the SCR normally varies from 0 to 1·25, a larger value indicating the severity of shear concentration on that particular wall; the BCR may vary from 0 for no bending concentration on the wall to 2 or above for critical cases.

The height-wise distributions of the SCRs and BCRs on the wall and column for model A are depicted in Figure 5. Owing to the symmetric geometry and gravity loads, equivalent results for only one of the walls and columns are presented. The average normal stress on the transfer level under a factored gravity load, $[\sigma_{N,\mathrm{total}}]_{1/F}$, is approximately 11 MPa, which is equivalent to an axial load ratio ($= N_i/A_i f_{\mathrm{ck}} \approx \sigma_{N,\mathrm{total}}/f_{\mathrm{ck}}$) of 0·3 for a RC wall made up of C45 concrete ($f_{\mathrm{cu}} = 45$ MPa), where f_{cu} and f_{ck} ($\approx 0\cdot8 f_{\mathrm{cu}}$) denote the characteristic cube and cylinder strength of concrete in MPa, respectively. For brevity the SCRs and BCRs of various floors are calculated using $\sigma_{N,\mathrm{total}}1/F$. The SCRs and BCRs increase from 0 at the fourth storey above the transfer level to the largest values of 0·34 and 1·4, respectively, at the first storey. This result implies that a maximum average shear stress of $11 \times 0\cdot34 = 3\cdot8$ MPa is acting on the upper shear wall which results from solely gravity loads. A maximum bending stress equal to $11 \times 1\cdot4 = 15\cdot5$ MPa is also acting on the extreme fibre of the wall section at the first storey. It should be noted that this critical shear stress demand can take up almost 70% of the maximum allowable design strength stipulated by most of the standards, as shown in Table 2. For the columns below the transfer level, the stress concentration effect diminishes from the top to bottom interfaces of the column, where the stress demands are relatively trivial. The results demonstrate that the shear concentration effect is severe but will be limited to a few storeys above the transfer level. The shear concentration zone could be associated with the deflection profile or the clear span, L, of the transfer structures. In order to study the intensity of the stress concentration on walls under various structural arrangements, maximum SCRs and BCRs induced at the wall–transfer interface are compared in the following study.

4.2 Shear concentration effect with varied support locations

In this section, the influence of the locations of the supporting columns on the SCR and BCR is studied. The locations of both supporting columns for model A and only the right side column in model B are altered to simulate various support conditions. Figure 6 depicts the variations of SCRs and BCRs for the walls and columns in model A. At the concentric support condition, where the offset distance = 0 m, the SCR and BCR are almost completely suppressed, indicating the optimal support conditions. Not surprisingly, when the supporting columns are shifted
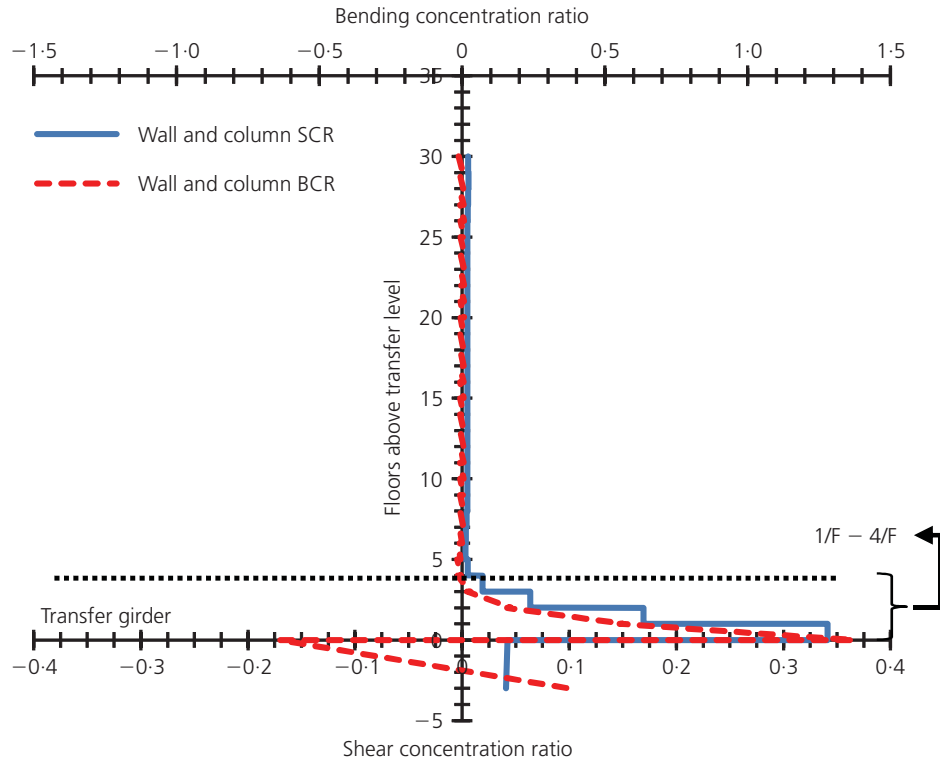
Structures and Buildings
Volume 168 Issue SB1

Gravity-induced shear force in reinforced
concrete walls above transfer structures
Tang and Su

Figure 5. Vertical distributions of shear and bending
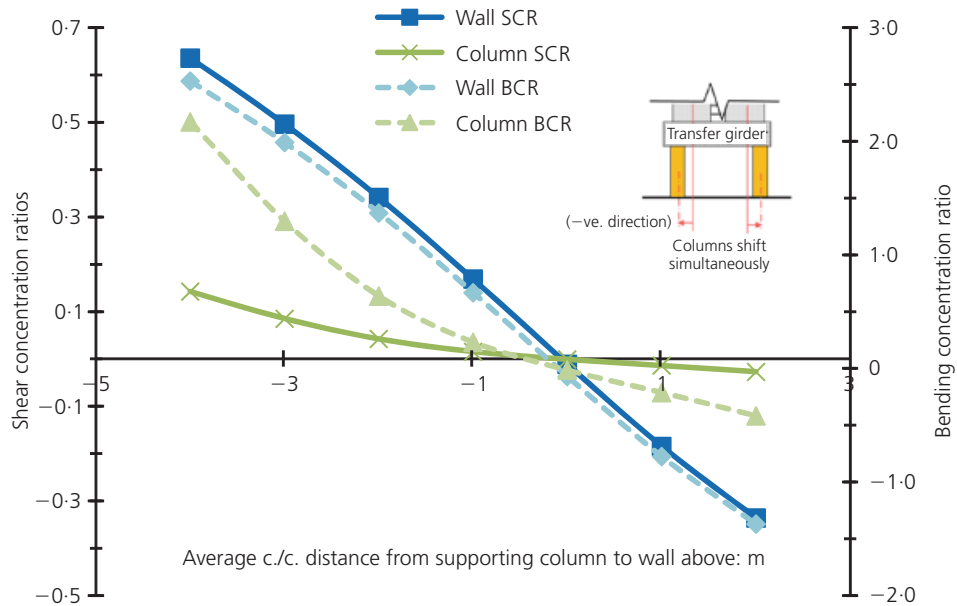concentration ratios for model A

Figure 6. The variations of shear and bending concentration
ratios against the locations of supporting columns for model A

symmetrically, the SCR and BCR for walls and columns increase
with larger offset distances in either direction. It should be noted
that the increasing rates of the SCR and BCR are almost the
same, such that the shear span ratio is close to a constant (M_i/V_i)

with all offset distances. The most critical SCR and BCR are
0·64 ($\sigma_{V,i} = 7·2$ MPa) and 2·5 ($\sigma_{M,i} = 28·6$ MPa), respectively,
when the offset distances for both walls are at −4 m (clear span
of column supports = 14 m). Even for a moderate offset dis-

Structures and Buildings
Volume 168 Issue SB1

Gravity-induced shear force in reinforced
concrete walls above transfer structures
Tang and Su

tance = −1 m (clear span of column supports = 8 m), the corresponding SCR and BCR are 0·17 ($\sigma_{V,i}$ = 1·9 MPa) and 0·67 ($\sigma_{M,i}$ = 7·5 MPa), respectively. With the support being shifted further inward, reversed shears and moments are induced on the walls and columns.

To minimise the stress concentration effect, the optimised location is the concentric support condition if there exists the same number of supports as the upper shear walls, such as in model A. However, it is more complex if there are fewer supports than the supported shear walls, as in model B. Figure 7 presents the variations of SCRs and BCRs for the interior wall and the cantilevered exterior wall (labelled in Figure 3) as a function of the offset distance of the right side column from that exterior wall. The optimised location for the minimum shear load is neither the concentric support conditions for the two walls (offset = 0 m and 4·5 m) nor the average of the two (offset = 2·25 m); it is at an offset distance close to 1·5 m. Nevertheless, the stress concentration effect cannot be completely eliminated as in model A; SCR = 0·15 ($\sigma_{V,i}$ = 1·7 MPa) remains on the inner wall. For other support conditions, the severe stress concentration on the cantilevered exterior wall can reach as high as SCR = 0·25 ($\sigma_{V,i}$ = 3·0 MPa). When the support is between the interior and cantilevered exterior walls with an offset distance from 2 to 4 m, reversed shear and moment loads are induced on the walls. The loads are attributed primarily to the actions and reactions formed when the walls rotate and deflect away in opposite directions above the deformed transfer girder. Since floor slabs and beams just above the transfer tend to restrict such deformation, critical tensile forces could develop. These explain the extensive cracks observed on the walls and slabs in Figure 1.

4.3 Shear concentration effect along the storey height
Earlier studies (e.g., Su and Cheng, 2008) have indicated that the effect of shear concentration owing to the transfer plate deformations under lateral or gravity loads is restricted to a few storeys above the transfer level. The above observation coincides with the elevation plots of the SCR and BCR for model A in Figure 5. For model B, a comparison of the shear and bending concentration ratio along the building height above the transfer level is shown in Figure 8. It can be noted that opposite SCRs and BCRs are induced on the interior and cantilevered exterior walls. The stress concentration effect diminished rapidly against an increase in floor levels. It almost completely vanishes at the fourth storey above the transfer level. The above results support the assumptions made in deriving the physical model proposed in Section 2.

4.4 Substitute model using gravity loads
In practical design, the typical floors are often omitted in the building model for the gravity analysis. They are substituted by the equivalent gravity loads. Hence, any amendments to the building layouts can easily be catered for, making it possible to rerun the analysis in a limited amount of time. However, an inappropriate model simplification could result in significant errors. In this study, different numbers of the typical floors above the transfer level are substituted by loading, and the corresponding SCR and BCR for the upper shear walls at the first floor are compared in Figures 9 and 10, respectively. With more storeys modelled above the transfer level, it is shown that the results converge with the full model analysis, which is shown as dashed lines in the figures.
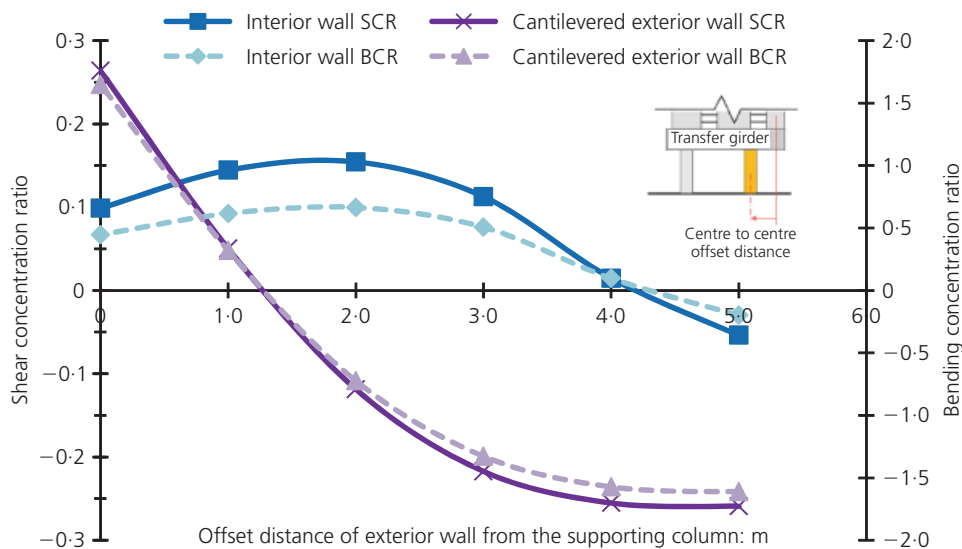

Figure 7. The variations of shear and bending concentration ratios against the offset distance of support for the cantilevered exterior wall in model B
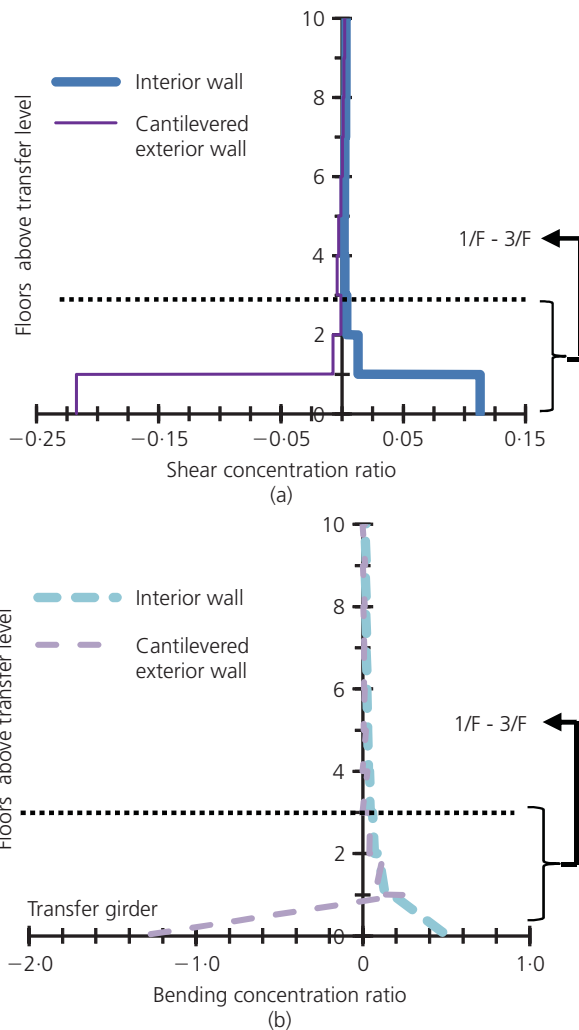
Figure 8. Vertical distributions of stress concentration ratios in (a) shear and (b) bending for model B
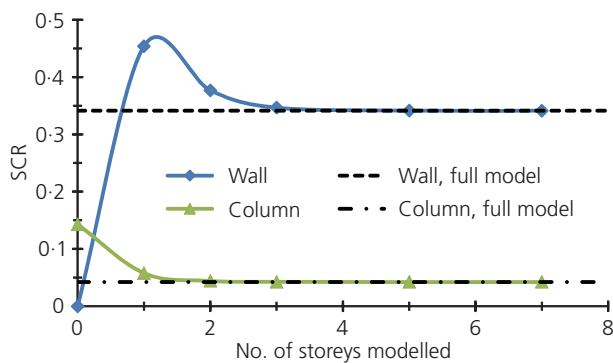

Figure 9. The variations of shear concentration ratios against the storeys modelled above the transfer girder for model A
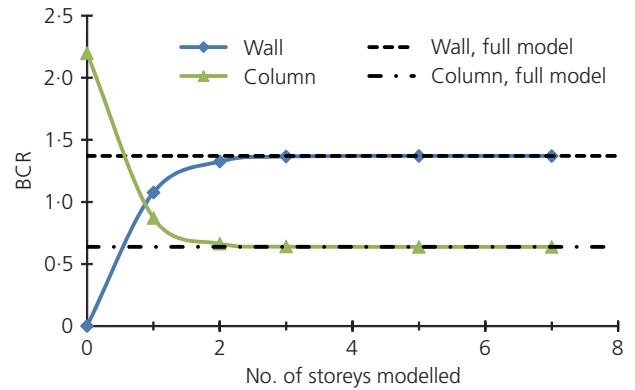

Figure 10. The variations of bending concentration ratios against the storeys modelled above the transfer girder for model A

In terms of load transfer, the omission of higher storeys above the transfer level results in shorter shear walls being modelled. As gravity loads are transmitted from the walls to the end column supports through the transfer girder, the concrete strut developed in the shear wall and transfer girder is also shortened. The smaller inclination angle of the strut to the horizontal leads to a less effective strut action. A higher SCR is induced to transmit the same amount of gravity load. In contrast, the complete omission of storeys above the transfer level inappropriately neglects the interacting strut or tie effect of floor slabs in higher storeys. The reduced moment arms outweigh the larger shear loads, leading to smaller base moments and an underestimated BCR in the upper shear walls. Comparatively, the BCRs on supporting columns are overstated by more than one time with no typical storey modelled. This is due to the less effective tie-and-strut action in transferring the loads from the upper shear walls to the end column, such that more loads are carried through the flexural beam action of the transfer girder, and the moment induced is carried down to the column. As a result, although typical floors above the transfer level could be simplified as equivalent gravity loads, at least two storeys above the transfer level should be modelled. The slabs and beams are essential for the interacting actions between walls above the transfer and should be modelled in the analysis.

4.5   Rigid diaphragm assumption
For the full model analysis, the rigid diaphragm assumption is often adopted to shorten the computational time. This assumption condenses all the degrees of freedom associated with the in-plane floor slab displacements. However, as mentioned in the last section, the coupling effect of slabs and beams on the walls is crucial and should be appropriately modelled. Although the in-plane deformation of the transfer girder is not affected, it is essential to release the rigid diaphragm assumption on storeys above the transfer level so as not to overstate the wall shear with over-rigid floor slab connections above the transfer level. Figure 11 illustrates the distribution of SCRs for model A with an increased number of storeys using flexible diaphragms above the
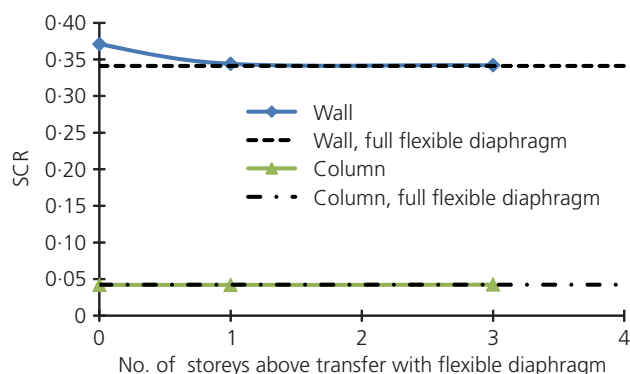
Structures and Buildings
Volume 168 Issue SB1

Gravity-induced shear force in reinforced
concrete walls above transfer structures
Tang and Su

Figure 11. The variations of shear concentration ratio against the storeys with flexible diaphragms above the transfer girder for model A

transfer level. It can be concluded that the rigid diaphragm assumption mainly affects the upper shear walls and that the result converges quickly with the first storey being released from such an assumption.

4.6 Stiffness degradation for structures undergoing non-linear behaviours

The above analyses are based on elastic analysis, which should suffice to model typical structures under gravity loads with limited non-linear behaviours. However, in critical cases, such as under a rare earthquake, the effects of stiffness degradation can significantly affect the predicted deformations (ACI 318–11 (ACI, 2011)), in particular the deformation-induced stress concentration discussed in this paper. Reduced flexural and shear stiffness following a few well-developed seismic codes (ACI 318–11, (ACI, 2011); ASCE41–06 (ASCE, 2007); Eurocode 8 (CEN, 2004)) have been considered to take into account the reduction in stiffness at the yield state. Table 5 summarises the effective stiffness at the yield state adopted in this study, where I denotes the gross sectional moment of inertia and G is the short-term shear modulus of the section. The study finds that, although the rotation at the base of upper walls could be drastically increased by 80%, the reduced stiffness of the walls can sufficiently compensate the effect, resulting in only a slight increase of about 10% in the SCRs. Comparisons of SCRs using full or yielded stiffness for model A and B are shown in Figure 12. Hence, the

	Flexural stiffness (EI)	Shear stiffness (GA)
Column	0·7	0·5
Wall	0·6	0·5
Slab	0·25	0·5
Beam	0·35	0·5
Transfer girder	0·35	0·5

Table 5. Effective stiffness adopted for various structural members under yield state

results deduced from the above analyses could be applicable to similar structures undergoing the yield state. In cases where cracking occurs only on the upper shear walls and the coupling beams under tie forces, more pronounced reductions in SCRs are obtained, which are limited to 15% and 30%, respectively, for models A and B.

From the perspective of seismic design, general performance criteria such as the inter-storey drift limit at the storey just above transfer level may have to be reduced to account for the base rotations of critical walls contributing to the actual racking deformation angle (CTBUH, 2008). For instance, the cl.8.7.1 in Peer (2010) and cl.3.5.4.2.1 in LATBSDC (2011) recommend the inter-storey drifts ≤ 3% for a building designed to the maximum considered earthquake (MCE) level. This limit serves to prevent the non-structural components from causing any life safety hazard as well as to protect the structural components. The two codes agree that structural elements with good detailing and proper yielding mechanism are capable of providing the 3% drift limit without severe strength degradation. If the strength degradation in these elements is more severe than the shear force induced by the P-delta effect. Slight perturbation could possibly result in instability or even progressive collapse of the structures. As a considerable amount of deformation, which could be associated with 2 to 3 MPa shear stress, is induced in the supported shear wall due to the warping of the transfer structure under gravity loads, it is reasonable to make reduction in the allowable inter-storey drift limit in the seismic design for storeys in the vicinity of the transfer structure.

4.7 Effects of sequential construction and creep

Sequential construction has received interest in most structures requiring special attention to ensure the structural integrity is not impaired throughout the different stages of construction, particularly for bridges and high-rise structures. In view of the stress concentration effect caused by deformation of the transfer structure – a prime cause of such effect being the total dead and imposed loads of the building – the sequence of loading from each storey would not significantly alter the SCRs and BCRs. Sequential construction of each storey has been modelled in Etabs. Figure 13 compares the SCRs and BCRs for models A and B with and without the consideration of sequential construction. The mild differences shown in SCRs and BCRs coincide with the postulation.

Upon completion of the construction of the building, the RC creeps with time under quasi-permanent loads. Significant creep strain, equivalent to several times the initial elastic strain, could develop. According to Model Code 2010 (Fib, 2010), the time-dependent strain should be accounted for in the stress calculation (cl.7.6.3) under service loads. The time-dependent strains comprise stress-dependent strains (initial and creep strains) and stress-independent strains (shrinkage and thermal strains), the latter of which are not discussed herein due to their reversible nature and cyclic fluctuations caused by seasonal rain and other
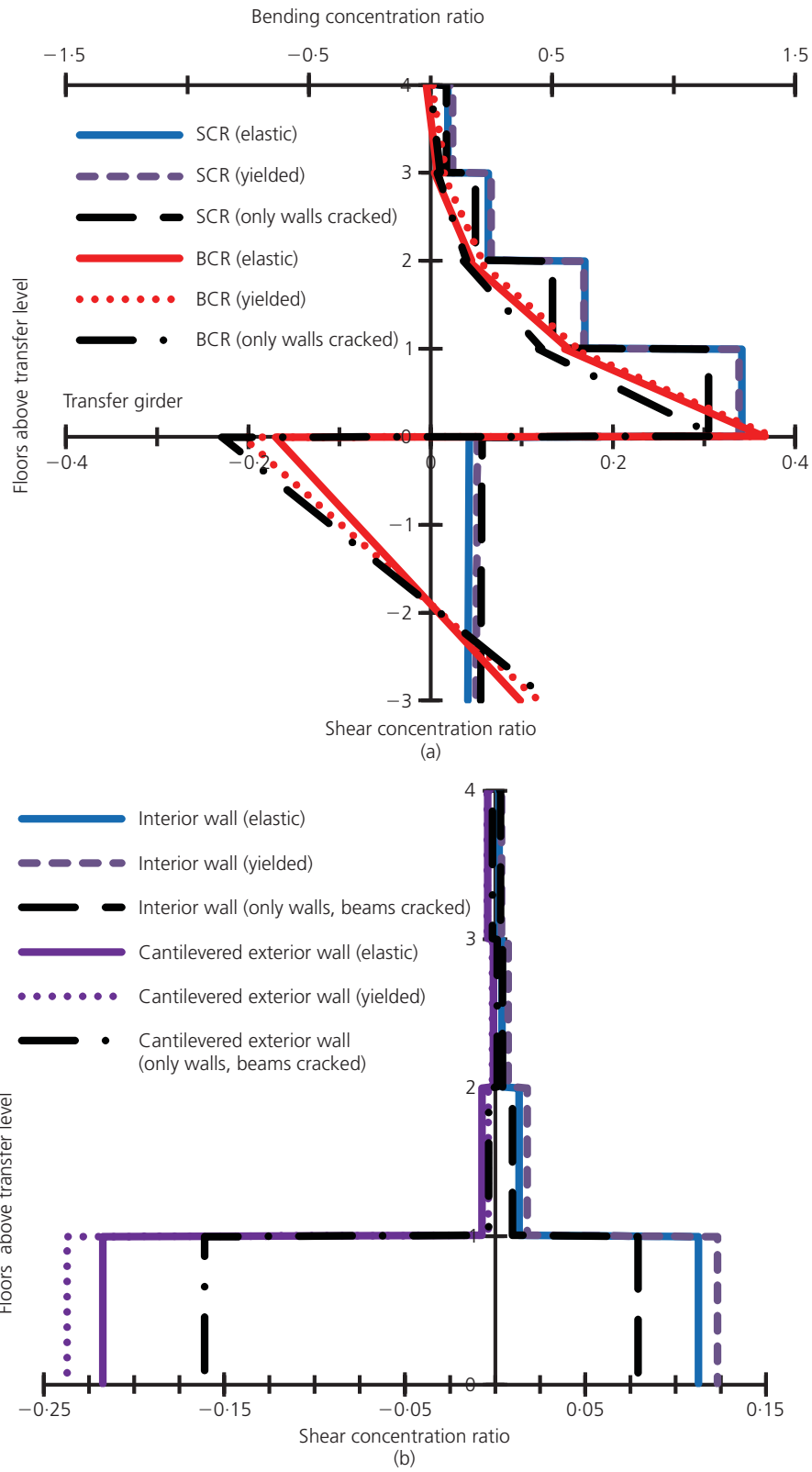
Structures and Buildings
Volume 168 Issue SB1

Gravity-induced shear force in reinforced
concrete walls above transfer structures
Tang and Su

Figure 12. The comparisons of the vertical distributions of
(a) BCRs and SCRs for model A and (b) SCRs for model B under
yield state or localised cracking of the upper walls and beams

Structures and Buildings
Volume 168 Issue SB1

**Gravity-induced shear force in reinforced
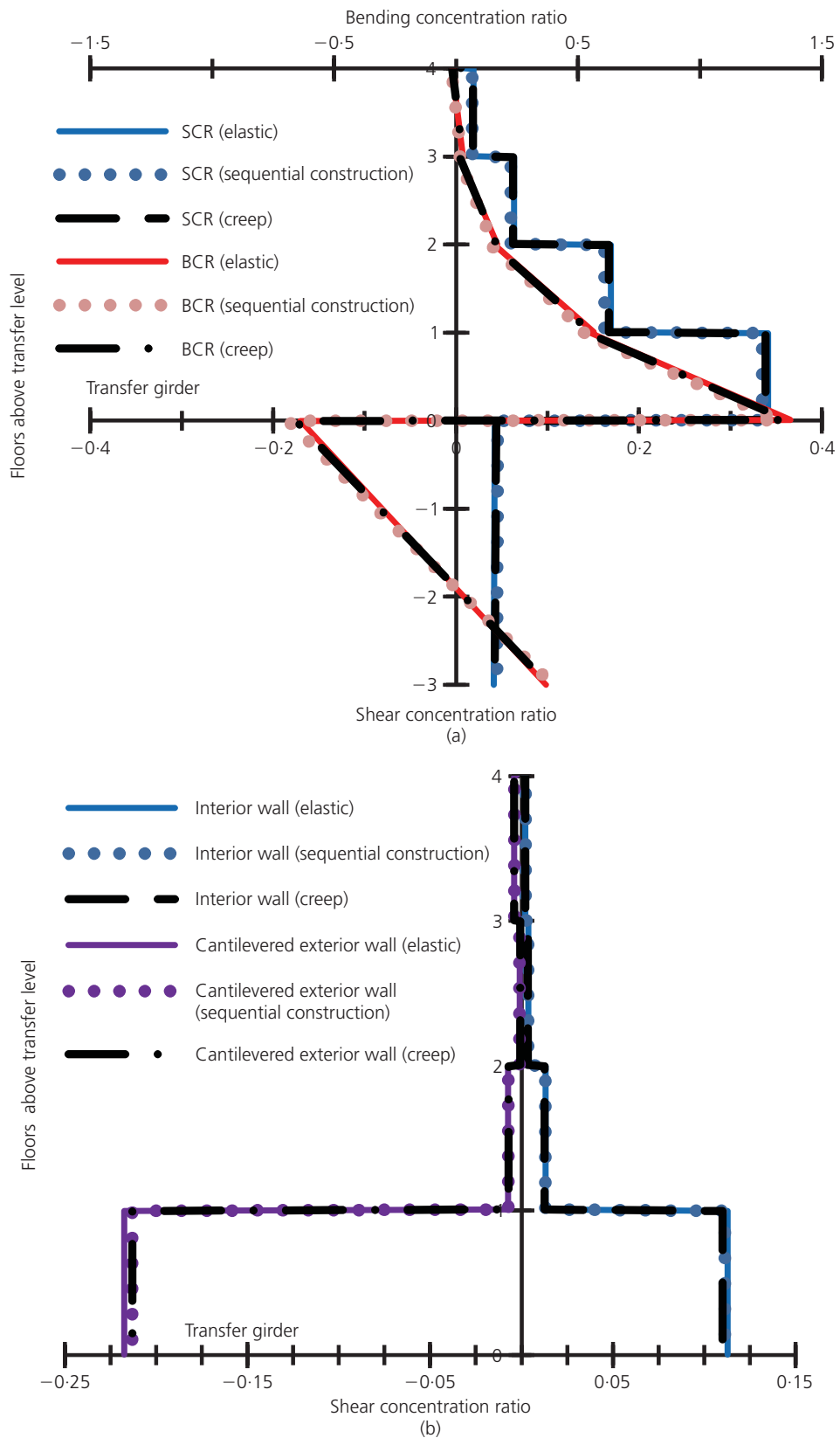concrete walls above transfer structures**
Tang and Su

Figure 13. The comparisons of the vertical distributions of
(a) BCRs and SCRs for model A and (b) SCRs for model B with
the effects of sequential construction or creeping of RC

Structures and Buildings
Volume 168 Issue SB1

Gravity-induced shear force in reinforced
concrete walls above transfer structures
Tang and Su

weather conditions (Park and Paulay, 1975). In compliance with cl.5.1.9.4 in Model Code 2010 (similar creep estimations are provided in cl.3.1.4 and Annex B of Eurocode 2, BSI, 2004), the stress-dependent strains – initial and creep strains – are calculated. Assuming normal-strength cement, mean cylinder strength of concrete ($f'_c = f_{ck} + 8$ MPa) = 44 MPa and humidity of 70% (normal in coastal cities, e.g. Hong Kong), the creep coefficients $\varphi(t, t_0)$ are estimated to be 0·90 for the transfer girder and supporting columns, 0·98 for the upper walls and 1·04 for the coupling beams (Eurocode 2, BSI, 2004). The creep coefficient denotes the equivalent initial strain (ε_0) to be developed by creeping from time t_0 (= 365 d, assuming the structure is fully loaded after completion) to t (= 10 000 d) under uniaxial stresses.

As the derivation of the creep strain is empirical, when neither the stochastic nature has been accounted for nor special measures have been taken to reduce the associated uncertainties, accurate structural analysis of the creep effect makes no sense (Bažant, 1988). For simplified analysis, the age-adjusted effective modulus of elasticity (AAEM) proposed by Bažant could be adopted. For brevity, the underlying concept is that the total strain of the RC component being loaded from time t_0 to time t (= 10 000 d) can simply be calculated by using the effective modulus, which is expressed as

5.
$$\Delta\varepsilon = \frac{1}{E''}B\Delta\sigma + B\sigma(t_0)\frac{\phi(t, t_0)}{E(t_0)} + \Delta\varepsilon_0$$

Age-adjusted effective modulus

6.
$$E'' = \frac{E(t_0) - R(t, t_0)}{\phi(t, t_0)}$$

where σ is the applied stress tensor, ε is the strain tensor, E is the short-term elastic modulus, B is the compliance tensor and Δ denotes the change of strain or stress from time t_0 to t. The age-adjusted effective modulus depends on a linear algebraic relaxation function $R(t,t_0)$. This modulus can be closely approximated by Equation 7 assuming the ageing coefficient $\chi(t,t_0) = 1$.

Effective modulus for a modified creep coefficient

7.
$$E'' = \frac{E(t_0)}{[1 + \chi(t, t_0)\phi(t, t_0)]}$$

For simplicity, the applied stress is assumed to be invariant: that is, the strain recovery due to stress relaxation is ignored. This assumption is verified later. In addition, the effective modulus that accounts for the effect of creep strain has been adopted in the Etabs model. When creep strains are developed to encompass whole structures, the effective moduli of 0·50 E for upper walls, beams and slabs, and 0·53 E for the supporting columns and the

transfer girder, are estimated from Equation 7. They differ mainly due to the effective thicknesses that constrain the moisture loss resulting in lower creep strain. Figure 13 depicts the SCRs and BCRs of models A and B when the creep strain is considered. The reductions in SCRs and BCRs are less than 5%, which is modest. This is attributed to compensation between the reduced lateral thrust by the coupling beam and the increase in the base rotations of the walls. The slight variations of SCRs and BCRs justify the invariant stress assumption in deriving the effective moduli.

As high compressive stress would result in high and almost unpredictable creep, a non-linear model should be used for creep assessment when concrete compressive stress $> 0·4 f'_c$ under service loads (cl.7.6.3.3 Fib, 2010). The current model under examination is subjected to an axial load ratio $\approx 0·2$ under service loads (i.e. load factor = 1·0). The stress at the extreme compressive fibre could be close to or exceed $0·4 f'_c$ if the bending stress (if BCR $\geqslant 1$) is considered. Yet, the above linear creep analysis defines the lower-bound benefit due to creep. A larger reduction in SCRs could be obtained if a detailed non-linear creep model was used. However, this may be justifiable for a realistic project in which actual structural layouts are also considered in detail.

4.8 Mitigating measures
To reduce the significance of the shear concentration effect on the upper shear walls, rather than changing the column layout to minimise the support offset, which is often constrained by various architectural requirements, other available solutions are discussed as follows.

(a) Use of late-cast slabs: As the shear concentration effect is attributable to the displacement of the supported walls and is transmitted through the coupling slabs and beams, the problem can be resolved if the walls can displace freely under gravity loads from full construction before the restraining slabs and beams are cast. Figure 14 illustrates the reduction in the SCR and BCR for model A with increased storeys using late-cast slabs. A significant amount (up to 30–40%) of
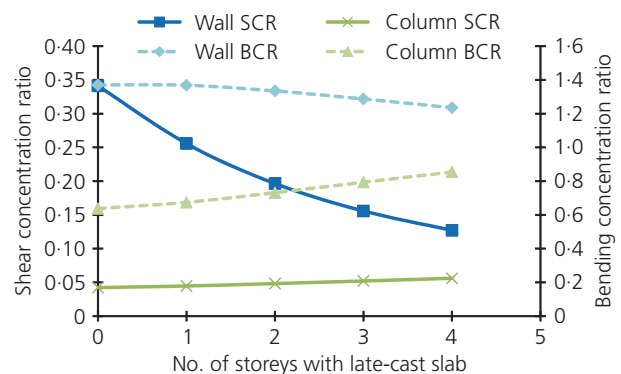

Figure 14. The variations of shear and bending concentration ratios against the storeys with a late-cast slab above the transfer girder for model A

Structures and Buildings
Volume 168 Issue SB1

Gravity-induced shear force in reinforced
concrete walls above transfer structures
Tang and Su

the shear stress on the upper shear walls can be reduced by
having the first and second floors use late-cast slabs.
However, the reduction in the BCR is less than 10%, which is
insensitive to this measure. This is most likely due to the
balanced effect between the increased moment arm and the
reduced shear loads on walls with late-cast slabs.

(b) Increase in the depth of the transfer girder: Increasing the
depth of the transfer girder could effectively control the
bending and shear deformations of the transfer girder. Figure
15 shows the variations of the SCR and BCR for model A
and B against increased depth of the transfer girder. To
reduce 50% of the SCR, the depth of the transfer girder is
increased from 2 m to 6 m for model A (span-to-depth ratio
from 5 to 1·7), whereas model B requires only half the depth,
which is 3 m (span-to-depth ratio from 1·5 to 1, considering
the span of the cantilever transfer girder). The more sensitive
result revealed in model B is likely attributable to the smaller
span length and the bending and shear deformations of the
transfer girder is counter-balanced by the eccentrically
supported interior wall and cantilevered exterior wall on
either side of the supporting column. A deeper transfer girder
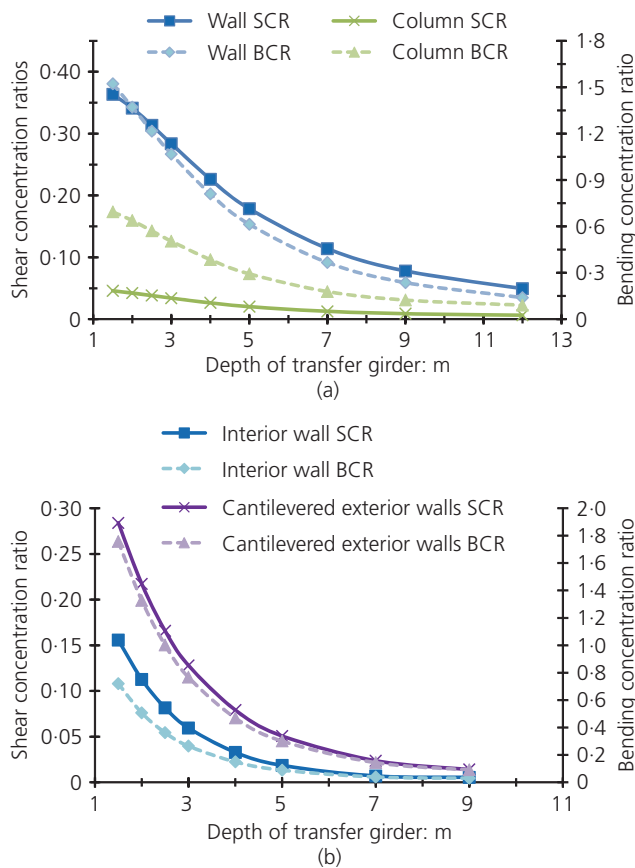has other merits, such as alleviating the local shear stress

induced within a wall and the shear concentration owing to
lateral loads by having a more robust transfer structure.

The remedial measures above are only for reference. As the
mechanism is well understood, the design philosophy is to reduce
the lateral stiffness of the coupled shear walls and/or increase the
vertical stiffness of the transfer girder; hence, this approach can
restrain the bending and shear deformations of the transfer girder
and the shear loads inflicted on the supported walls. More
alternatives could be available depending on the site conditions,
such as (a) shortening the wall length by using more wall panels,
in which discrete and slender wall segments reduce the lateral
stiffness and hence the shear loads induced under a constant
displacement; (b) using higher grade concrete for a few storeys
around the transfer level, the maximum shear capacity can be
increased by 20–30% by changing from C45 to C60 concrete,
depending on the code provisions; and (c) increasing the thickness
of shear walls above the transfer structure. Although the SCR and
BCR are insensitive to the change in the axial normal stress, the
absolute shear stress is linearly proportional to the normal stress
on the wall. Figure 16 presents the variations of the SCRs and the
average normal stress ($\sigma_{N,total}$) with various shear wall thicknesses.

5. Conclusion

Owing to the critical shear concentration effect on shear walls
above column-supported transfer girder structures, a critical
proportion of the maximum allowable shear strength (30–50%)
could be consumed solely due to gravity loads. Two-dimensional
elastic models effectively illustrate the proposed shear concentra-
tion mechanism of the shear walls above a deformed transfer
girder under in-plane gravity loads. Despite reduction in shear by
15 to 30% with localised cracking of the upper shear walls,
almost unchanged shear loads revealed on structures with yielded
stiffness or under long-term creeping prove the applicability of
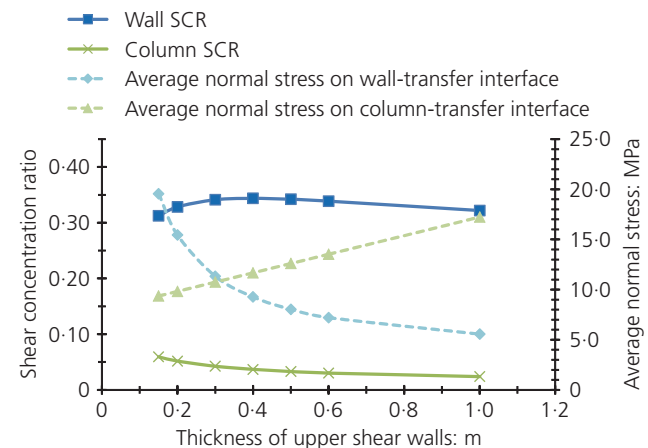this study to those conditions.

Figure 15. The variations of shear and bending concentration
ratios against the depth of the transfer girder for (a) model A and
(b) model B

Figure 16. The variations of shear concentration ratios and
average normal stresses against the thickness of the upper shear
walls for model A

Structures and Buildings
Volume 168 Issue SB1

Gravity-induced shear force in reinforced
concrete walls above transfer structures
Tang and Su

To appropriately account for the shear concentration effect, not only does special attention have to be placed on modelling techniques, such as the release of the rigid diaphragm assumptions above the transfer level and the limit of simplified models by equivalent gravity loads, but it is also crucial to optimise the structural layout to minimise the bending and shear deformations of transfer girders and hence the difference in base rotations between adjacent shear walls. If, due to architectural constraints, optimised support conditions are not possible, other remedial measures are proposed, such as using late-cast slabs, transfer girders with increased depth, segmented and thicker upper shear walls, and concrete of higher grade for critical regions.

REFERENCES

ACI (American Concrete Institute) (2011) ACI 318–11: Building code requirements for structural concrete and commentary. ACI, Farmington Hills, MI, USA.

ASCE (The American Society of Civil Engineers) (2007) ASCE 41–06: Seismic rehabilitation of existing buildings. ASCE, Reston, VA, USA.

Bažant ZP (1988) *Mathematical Modeling of Creep and Shrinkage of Concrete*. Wiley, New York, NY, USA, Rilem TC69 Committee.

BSI (1997) BS8110: The structural use of concrete: Part I, code of practice for design and construction. BSI, London, UK.

BSI (2004) BS EN 1992–1-1: 2004: Eurocode 2: Design of concrete structures – Part 1: General rules and rules for buildings. BSI, London, UK.

CEN (European Committee for Standardisation) (2004) EN 1998–1: 2004: Eurocode 8: Design of structures for earthquake resistance – Part 1: General rules, seismic actions and rules for buildings. CEN, Brussels, Belgium.

Choo BS and Li GQ (1997) Structural analysis of multi-stiffened coupled shear walls on flexible foundations. *Computers and Structures* **64(1–4)**: 837–848.

CSI (Computers and Structures, Inc.) (2005) *CSI Analysis Reference Manual For SAP2000, ETABS, and SAFE*. CSI, Berkeley, CA, USA.

Coull A (1971) Interaction of coupled walls with elastic foundations. *American Concrete Institute* **68(6)**: 461–456.

Coull A and Chantaksinopas B (1974) Design curves for coupled shear walls on flexible bases. *Proceedings of the Institution of Civil Engineers* **57(4)**: 595–618.

CSA (2004) CSA, A23.3–04: Design of concrete structures. Canadian Standards Association (CSA), Ontario, Canada.

CTBUH (2008) *Recommendations for Seismic Design of High-Rise Buildings*. Council of Tall Buildings and Urban Habitat (CTBUH), Chicago, IL, USA.

Fib (International Federation for Structural Concrete) (2010) *Model Code 2010 Vol 1 and Vol 2*. Ernst & Sohn, Germany, fib Bulletin No. 55 and 56. Fib, Lausanne, Switzerland, Fib Special Activity Group 5, DCC Document Competence Center Siegmar Kästl e. K.

Kuang JS and Zhang Z (2003) Analysis and behaviour of transfer plate-shear wall systems in tall buildings. Design of tall and special buildings. *The Structural Design of Tall and Special Buildings* **12(5)**: 409–421.

LATBSDC (Los Angeles Tall Buildings Structural Design Council) (2011) *An Alternative Procedure for Seismic Analysis and Design of Tall Buildings Located in the Los Angeles Regions*. LATBSC, Los Angeles, CA, USA.

Liu K and Wang L (2009) Crack control during construction of high-rise RC transfer structures. *Sichuan Building Materials* **35(3)**: 55–55 (in Chinese).

Macleod IA and Green DR (1973) Frame idealization for shear wall support systems. *The Structural Engineer*, **51(2)**: 71–74.

Man CF (2010) Cracking in high-rise RC transfer structures. *Modern Business Trade Industry* **16(19)**: 379–380 (in Chinese).

Nadjai A and Johnson D (1998) Elastic and elasto-plastic analysis of planar coupled shear walls with flexible bases. *Computers & Structures* **68(3)**: 213–229.

Peer (Pacific Earthquake Engineering Research Center) (2010) *Guidelines for Performance-Based Seismic Design of Tall Buildings*. The TBI Guidelines Working Group, Berkeley, CA, PEER Report 2010/05.

Park R and Paulay T (1975) *Reinforced Concrete Structures*. Wiley, New York, NY, USA.

SNZ (Standards New Zealand) (2006) NZS 3101: Part 1: 2006: Concrete structures standard Part 1 –The design of concrete structures. SNZ, Wellington, New Zealand.

Stafford Smith B and Riddington JR (1977) The composite behaviour of elastic wall-beam systems. *Proceedings of the Institution of Civil Engineers* **63(2)**: 377–391.

Su RKL, Chandler AM, Lee PKK, To A and Li JH (2003) Dynamic testing and modelling of existing buildings in Hong Kong. *The HKIE Transactions* **10(2)**: 17–25.

Su RKL and Cheng MH (2008) Earthquake induced shear concentration in shear walls above transfer structures. *The Structural Design of Tall and Special Buildings* **18(6)**: 657–671.

Toutanji HA (1997) The effect of foundation flexibility on the interaction between shear walls and frames. *Engineering Structures* **19(12)**: 1036–1042.

Vuddandam RB, Toutanji H and Rodgers R (2013) Approximate solutions to coupled shear walls on fixed and flexible foundations. *Modern Applied Science* **7(4)**: 1–16.

WHAT DO YOU THINK?

To discuss this paper, please email up to 500 words to the editor at journals@ice.org.uk. Your contribution will be forwarded to the author(s) for a reply and, if considered appropriate by the editorial panel, will be published as a discussion in a future issue of the journal.

Proceedings journals rely entirely on contributions sent in by civil engineering professionals, academics and students. Papers should be 2000–5000 words long (briefing papers should be 1000–2000 words long), with adequate illustrations and references. You can submit your paper online via www.icevirtuallibrary.com/content/journals, where you will also find detailed author guidelines.